Investigation Of The Performance Of A Horizontal Axis Wind Turbine With The Use Of Blade Element Momentum Theory And CFD Computations

Conference Paper · March 2014

CITATION
1

READS
608

3 authors, including:

Georgios Martinopoulos
International Hellenic University
60 PUBLICATIONS **1,542** CITATIONS
SEE PROFILE

Dimitris Missirlis
Technological Educational Institute of Central Macedonia at Serres
67 PUBLICATIONS **856** CITATIONS
SEE PROFILE

INVESTIGATION OF THE PERFORMANCE OF A HORIZONTAL AXIS WIND TURBINE WITH THE USE OF BLADE ELEMENT MOMENTUM THEORY AND CFD COMPUTATIONS

E. Dimitriadis
School of Science and Technology,
International Hellenic University
e.dimitriadis@ihu.edu.gr

D. Missirlis
Lab. of Fluid Mechanics and Turbomachinery,
Aristotle University of Thessaloniki
misirlis@eng.auth.gr

G. Martinopoulos
School of Science and Technology,
International Hellenic University
g.martinopoulos@ihu.edu.gr

Abstract

The present work focuses on the comparison of the capabilities of Blade Element Momentum Theory (BEMT) in relation to Computational Fluid Dynamics (CFD) modelling when both methods are used for the design and performance optimization of a Horizontal Axial Wind Turbine (HAWT). Initially, a two-dimensional analysis and flow field investigation of the wind turbine blade profile was performed and the results were assessed in relation to available experimental data regarding lift and drag coefficients for various angles of attack.

Furthermore, a three-dimensional analysis was performed where the performance of the wind turbine blade design was at first, obtained with the use of BEMT. The same wind turbine blade design was then incorporated in a detailed 3D CFD model and the results were compared to those of BEMT.

The comparison revealed the superior performance and advantages of CFD modelling in relation to BEMT as CFD modelling could provide results with better agreement in relation to experimental data and a detailed view of the 3D flow field development and wind turbine blade-flow interaction, which are critical parameters for the optimization of wind turbine performance, and which cannot be obtained by BEMT.

Keywords: CFD, BEMT, Wind turbine.

1. Introduction

Aiming at increasing the use of renewable energy sources, efforts are constantly being made for the optimization of wind turbines. Toward this direction the investigation of wind turbine aerodynamics is of significant importance.

Such an effort is presented in this work where the aerodynamic performance of a wind turbine based on a NACA4415 airfoil is investigated with the combined use of the open source wind turbine calculation software QBlade v0.51 which is based on BEMT [1, 2], and CFD computations with k-ω Shear Stress Transport (SST) [3] and Reynolds Stress (RSM) [4] model. The selection of both approaches (i.e. BEMT and CFD) was based on the different advantages and disadvantages that each approach presents.

BEMT analysis can provide a fast approach for the basic analysis and design of a wind turbine blade, while CFD can provide a 3D detailed view of the flow field development during the operation of a wind turbine, capturing secondary flow phenomena which cannot be resolved during BEMT analysis, and which are necessary for optimizing the wind turbine blade design, although computations are more time consuming. For these reasons, a noticeable number of works is presented in international literature using BEMT method [5, 6] or CFD computations [7, 8, 9] for the analysis of wind turbines performance.

At the present work the results of BEMT together with CFD computations with k-ω SST and RSM turbulence models implemented in Ansys CFX software [10] were used in order to examine the aerodynamic performance of a wind turbine based on a NACA4415 airfoil for angles of attack between -10° and 20°.

The results were validated against experimental results presented in the work of Ostowari and Naik [11] which presents data from the investigation of an untwisted constant chord blade using NACA4415 airfoil through experimental

measurements in a wind tunnel. The measurements were carried out for blade aspect ratios of 6, 9, 12 to infinity and Reynolds number of $0.5x10^6$ to $1x10^6$ while the experimental data corresponding to Reynolds number of $0.75x10^6$ and aspect ratio of infinity were used for validating the results of the 2D computations.

At this point it must be mentioned that regarding the BEMT calculations, the effect of the airfoil design is taken into account by the calculation of the lift and drag coefficients which is performed by the XFOIL design analysis code [12, 13] which is integrated in the open source software QBlade, developed by Department of Experimental Fluid Mechanics from the Berlin Technical University.

2. 2D Computational modelling

For the 2D analysis a computational domain containing only a 2D cross section of the NACA4415 airfoil was created. The boundary conditions which were applied are shown in Figure 1.

At the inlet of the computational domain the velocity components were provided, together with turbulence intensity value. At the outlet of the computational domain, ambient static pressure was imposed. The bottom and top limits of the computational domain were given a translational periodic connection so as to use the same computational grid and setup for varying angles of inlet velocity without having to recreate the computational grid.

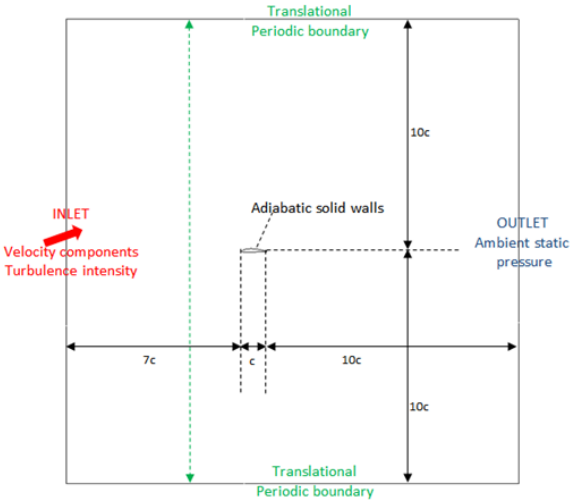

Figure 1: 2D CFD model boundary conditions

At the next step, the computational grid was created, as presented in Figure 2, taking into consideration the regions near the airfoil surface where significant flow variations were expected due to boundary layer development and possible flow separation regions.

In these regions, a much denser grid was created in order to resolute properly all phenomena of the flow field. In addition, as both turbulence models (SST and RSM) are Low-Re models, it was necessary to ensure that the non-dimensional y+ value for the first computational node from wall surfaces was less than 1.

After some initial attempts, a computational grid of approx. 330,000 nodes was created which could provide sufficiently grid independent results.

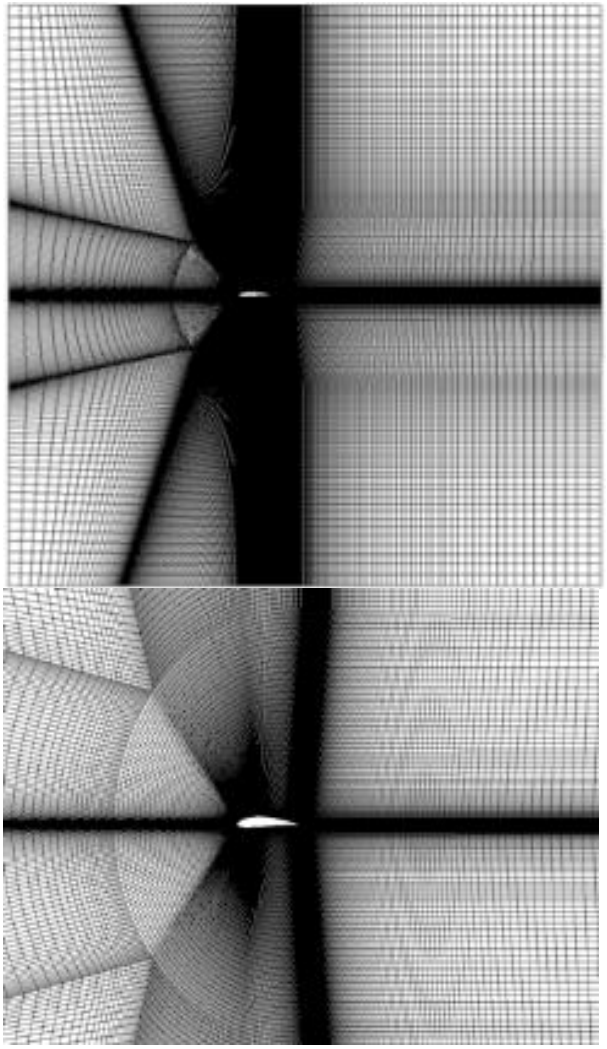

Figure 2: Computational grid

The conditions selected for the computations are presented in Table 1.

Reynolds number **Re**	750,000
Air density **ρ**	1.185 kg/m
Air dynamic viscosity **μ**	$18.31*10^{-6}$ kg/(m*s)

Table 1: Parameters of simulations

Based on the above values the relative air velocity ***W*** was calculated as:

$$Re = \frac{\rho W c}{\mu} \quad (1)$$

where c represents the airfoil chord length and was equal to 1 m. The calculation gives a relative velocity ***W*** of 11.48m/s.

The lift and drag coefficients were calculated as follows:

$$C_l = \frac{L}{0.5\rho W^2 c} \quad (2)$$

$$C_D = \frac{D}{0.5\rho W^2 c} \quad (3)$$

The 2D computations were performed for angles of attack ranging from -10° to 20°. Lift and drag coefficients were also calculated using XFOIL code integrated in QBlade.

The results are presented in Figure 3.

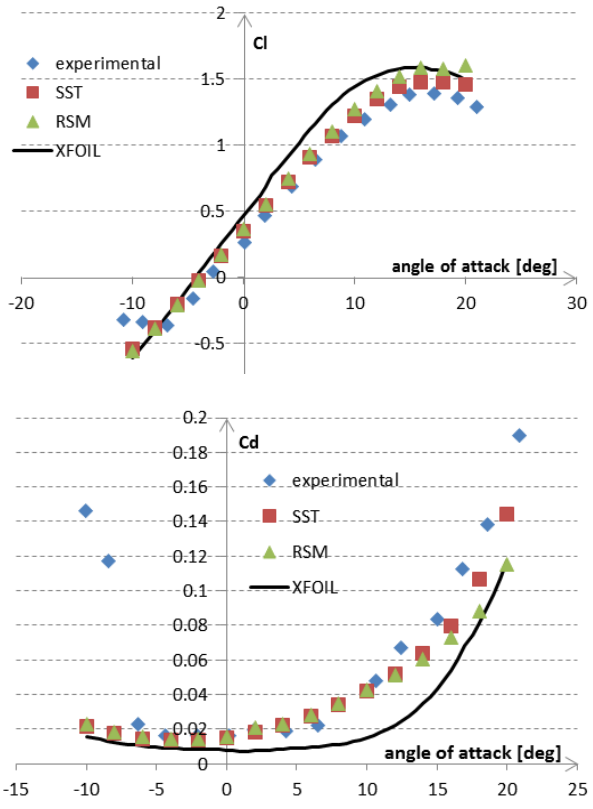

Figure 3: Lift and drag coefficient for various angles of attack

As it is apparent from Figure 3, the results of the SST turbulence model are closer to the experimental values than the ones of the RSM turbulence model for both lift and drag coefficients.

The results of XFOIL show increased deviation from the experimental data for both cases as XFOIL calculations which is mainly based on panel methods, show decreased accuracy in relation to CFD computations for conditions were viscous effects are particularly dominant i.e., close to stall conditions. The maximum lift to drag ratio appears for an angle of attack of 6°.

3. 3D Computational modelling

At the next step, a 3D design of the wind turbine blade was performed using QBlade based on the NACA4415 airfoil polar values obtained through XFOIL calculations.

The blade was designed and optimized using thirty sections, having a length equal to 2 m and a hub radius of 0.2 m, as presented in Table 2.

X (mm)	X/R	Chord (mm)	Twist angle (deg)
0	0.00	200	0
28	0.01	200	0
56	0.03	200	0
113	0.06	376	20.66
169	0.09	318	16.43
226	0.11	276	13.07
282	0.14	244	10.36
339	0.17	218	8.14
395	0.20	197	6.29
452	0.23	180	4.73
565	0.28	154	2.24
678	0.34	134	0.36
791	0.40	119	-1.12
904	0.45	107	-2.30
960	0.48	101	-2.82
1,017	0.51	97	-3.28
1,073	0.54	92	-3.70
1,130	0.57	88	-4.09
1,243	0.63	81	-4.78
1,300	0.65	78	-5.09
1,356	0.68	76	-5.37
1,469	0.74	70	-5.88
1,525	0.77	68	-6.11
1,582	0.80	66	-6.33
1,638	0.82	64	-6.53
1,695	0.85	62	-6.72
1,751	0.88	60	-6.90
1,808	0.91	59	-7.07
1,898	0.95	56	-7.33
1,988	1.00	54	-7.56

Table 2: Parameters for blade design

The 3D blade design was mounted on a typical wind turbine nacelle geometry and a 3D CFD model of a 120° sector with 1.3 million nodes was created in CFX, as presented in Figures 4 and 5.

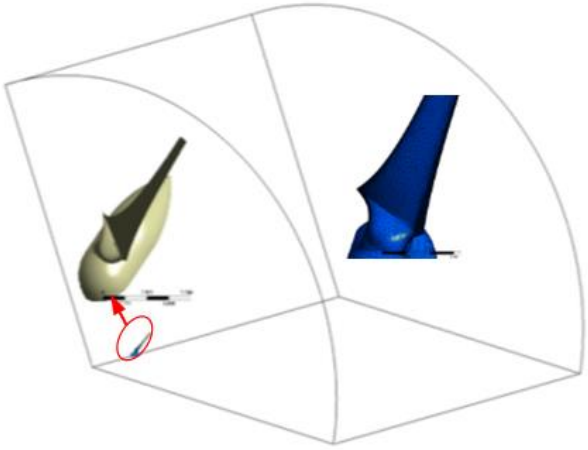

Figure 4: Computational domain for the 3D simulations

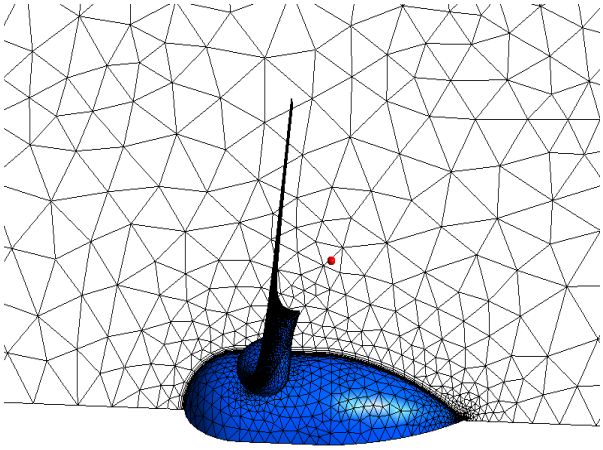

Figure 5a: Grid used for the 3D simulations

The 3D CFD computations were performed only with the SST turbulence model as this was the model showing the best performance in the 2D computations and also for time economy.

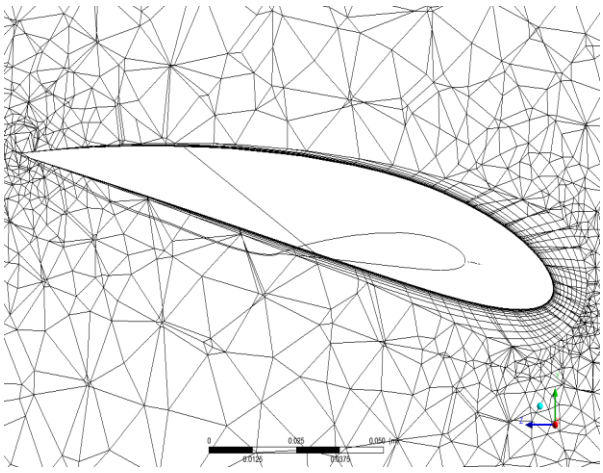

Figure 5b: Grid used for the 3D simulations

Similarly to the 2D approach, special care was provided so that the outside boundaries of the computational domain were placed significantly far from the wind turbine surface.

At the inlet of the computational domain the velocity components were provided (at the stationary frame of motion), together with turbulence intensity. The wind velocity was selected as 7.6 m/sec. At the outlet of the computational domain, ambient static pressure was imposed. The side boundaries of the computational domain were given a rotational periodic connection of 120° in order to incorporate the effect of the presence of the three wind turbine blades. The blade walls were rotating with a rotational speed of 4 rad/s which lead to a blade tip speed ratio of 7.

At the wind turbine surface, a non-slip wall boundary condition was applied since the computations were performed as steady in a rotating frame of motion, in relation to which the wind turbine surface is considered stationary.

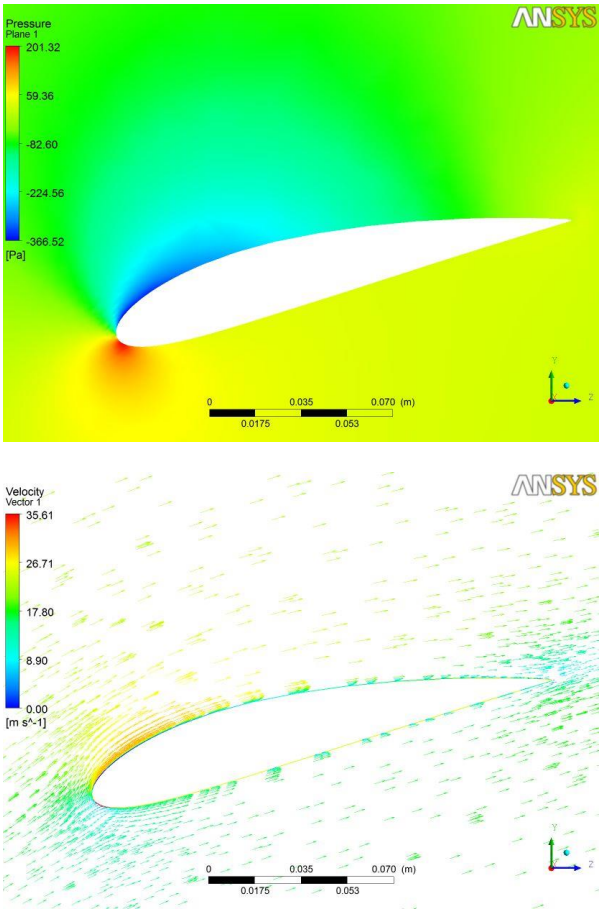

Figure 6: Static pressure contour plots and velocity vectors for a 0.65m cross section distance from the center of rotation

Finally, at the outside cylindrical surface of the computational domain undisturbed flow velocity condition was prescribed.

For the regions near the wind turbine surface where significant flow variations are expected due to the boundary layer development and possible flow separations, a denser grid was used so as to properly capture major flow field phenomena.

Since the SST Low-Re model was used, it was necessary to ensure that the non-dimensional y+ value for the first computational node from wall surfaces was less than 1.

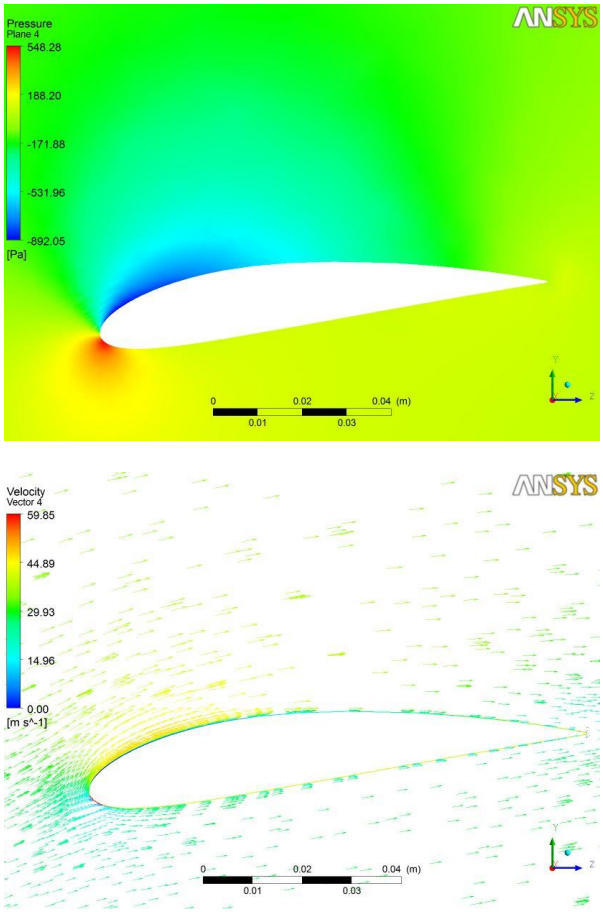

Figure 7: Static pressure contour plots and velocity vectors for a 1.15m cross section distance from the center of rotation

For this reason, grid inflation was applied on the wind turbine blade surfaces. The wind turbine blade was placed on a 6° angle of attack orientation (at the tip) since the twist angle of the blade was optimized for the maximum value of the lift to drag ratio.

Typical plots of the CFD solution are presented in Figure 6 to 8.

As it can be seen the flow remains fully attached along the blade length.

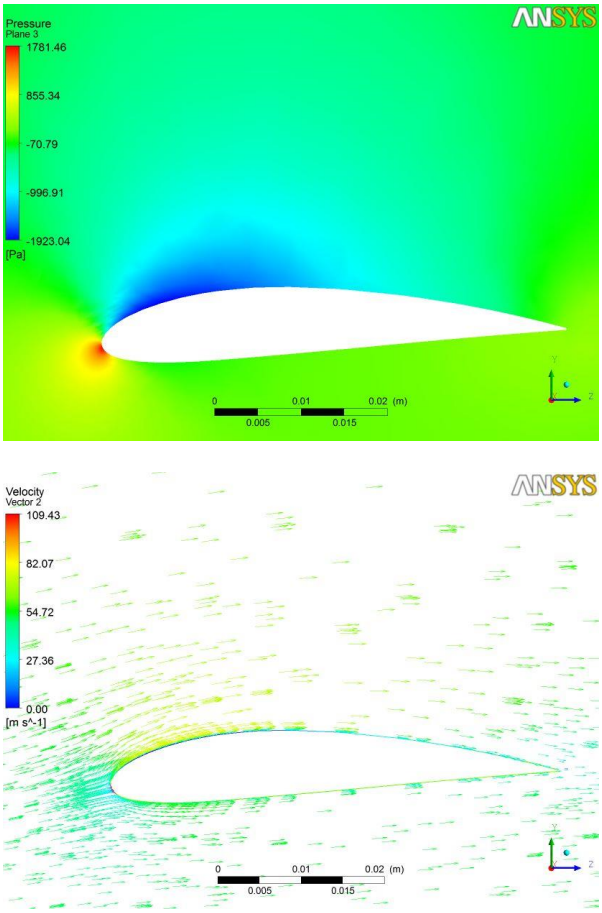

Figure 8: Static pressure contour plots and velocity vectors for a 2.15m cross section distance from the center of rotation

In order to evaluate the performance of the wind turbine, the power coefficient (ratio of power extracted by to wind turbine to the available energy of the wind) was computed.

The result of the 3D CFD computation is compared with the values obtained for various tip speed ratios using the BEMT method of QBlade, as shown in Figure 6.

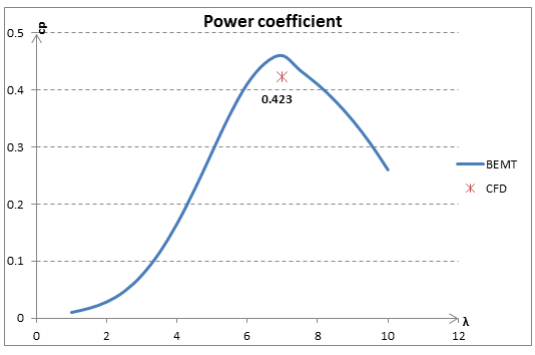

Figure 6: Power coefficient comparison between BEMT and CFD

As it can be seen, QBlade overestimates the power produced by the wind turbine, an assumption which can be primarily attributed to the overestimation of the lift coefficient calculated through XFOIL, the values of which are used by QBlade in BEMT method.

4. Conclusions

At the present work the flow field and the performance of a wind turbine blade was investigated with the contribution of CFD computations and BEMT method calculations.

The most significant conclusions are that CFD computations can accurately compute the flow around an airfoil. The point where stall begins can also be satisfactory predicted using CFD. The SST turbulence model has presented better results than the RSM turbulence model when compared with experimental data. In addition CFD results provide a detailed inside view in the flow field which can be significant for optimization purposes, especially for 3D computations.

The comparison between XFOIL values and CFD results for the lift and drag coefficients, reveals the weakness of XFOIL in order to perform satisfactorily for conditions were viscous effects are particularly dominant i.e., close to stall conditions. In general, the results of XFOIL tend to overestimate the lift coefficient values.

The power extracted from the wind for the selected conditions was calculated. A comparison with the values produced from the implementation of BEMT method through QBlade was achieved. The results show that the BEMT method overestimates peak power mainly as the outcome of the effect of XFOIL overestimation on lift coefficient values.

Both approaches can be helpful since they can be combined in an optimization strategy where the basic design can be performed with BEMT method, while the design fine tuning and optimization can be performed at the next stage through detailed 3D CFD computations.

References:

[1] QBlade Guidelines v 0.5. David Marten, (2012), TU Berlin

[2] QBlade: An open source tool for design and simulation of horizontal and vertical axis wind turbines, International Journal of Emerging Technology and Advanced Engineering, (2013), Vol. 3, pp. 264-269

[3] Menter, F.R., Two-equation eddy-viscosity turbulence models for engineering applications, AIAA-Journal.,(1994), Vol. 32(8), pp. 1598-1605

[4] Launder, B.E., Reece, G.J. and Rodi, W., Progress in the developments of a Reynolds-stress turbulence closure, J. Fluid Mechanics, (1975), Vol. 68, pp.537-566

[5] Tenguria, N, Mittal, N D and Ahmed, S., Investigation of blade performance of horizontal axis wind turbine based on blade element momentum theory (BEMT), International Journal of Engineering (2010), Vol. 12, pp. 25-35

[6] Rajakumar, S, Ravindran, D., Iterative approach for optimizing coefficient of power, coefficient of lift and drag of wind turbine. Renewable Energy (2012), Vol. 38, pp.83-93

[7] Yao, J., Yuan, W., Wang, J., Xie, J., Zhou, H., Peng, M., Sun, Y., Numerical simulation of aerodynamic performance for two dimensional wind turbine airfoils. Procedia Engineering (2012), Vol. 31, pp. 80-86

[8] Singh, K., Ahmed, M. R., Zullah, M.A. Lee, Y.-H., Design of low Reynolds number airfoil for small horizontal axis wind turbines. Renewable Energy (2012), Vol. 42, pp. 66-76

[9] Thumthae, C., Chitsomboon, T., Optimal angle of attack for untwisted blade wind turbine. Renewable Energy (2009) Vol. 34, pp. 1279-1284

[10] ANSYS CFX Documentation

[11] Ostowari, C., Naik, D., Post stall studies of untwisted varying aspect ratio blades with an NACA 4415 airfoil section-part I. Wind Engineering (1984) Vol. 8, pp. 186-194.

[12] Deperrois, A., XFLR5 - Analysis of foils and wings operating at low reynolds numbers, (2009)

[13] Drela, M. Youngren, H., XFOIL 6.94 User Guide, MIT Aero & Astro, (2001)